Sonochemical Preparation of Supported Hydrodesulfurization Catalysts

N. Arul Dhas, Arash Ekhtiarzadeh, and Kenneth S. Suslick*

Contribution from the School of Chemical Sciences, University of Illinois at Urbana-Champaign, 600 South, Mathews Avenue, Urbana, Illinois 61801

Received February 26, 2001

Abstract: Sonochemical preparation of Co and Ni promoted MoS_2 supported on alumina was achieved by high-intensity ultrasonic irradiation of isodurene solutions containing molybdenum carbonyl, dicobalt octacarbonyl, elemental sulfur, and Al_2O_3 or Ni−Al_2O_3 under Ar flow. The sonochemically prepared catalysts were characterized by elemental analysis, XPS, SEM, TEM, and XEDS, and hydrodesulfurization (HDS) activity evaluated for thiophene and dibenzothiophene substrates. The TEM studies on the sonochemically prepared catalysts indicate the formation of layered hexagonal MoS_2 (lattice fringes ∼6.2 Å) on the alumina support. The sonochemically prepared Co−Mo−S/Al_2O_3, Ni−Mo−S/Al_2O_3, and Co−Ni−Mo−S/Al_2O_3 are extremely active catalysts for the HDS of thiophene and dibenzothiophene, with activities severalfold those of comparable commercial catalysts under identical conditions. The layered structure of MoS_2 remained intact after 120 h of HDS, and the catalyst is reusable.

Introduction

Removing heteroatoms, especially sulfur, from petroleum constituents has always been an integral part of petroleum processing.[1] In a recent EPA regulatory change,[2] a 10-fold reduction in fuel sulfur emission makes the need for improved hydrodesulfurization (HDS) catalysts urgent. Alumina-supported molybdenum sulfide promoted with cobalt or nickel has been for several decades the catalyst of choice for hydrodesulfurization of fossil fuels due to its remarkable activity.[1,3−12] The MoS_2 basal plane is largely inert, while the edges of the MoS_2 layer expose Mo atoms for reaction.[13] Therefore, the catalytic activity is strongly dependent on the specific dispersion of the MoS_2 crystal (i.e., the ratio of edge sites to basal plane area) and on the local environment of the active edge sites. Detailed XAS studies suggest that Co in this structure decorates the edges of MoS_2 slabs and is coordinated to five sulfur atoms in a square pyramidal geometry in the (1 0 −1 0) edge planes of MoS_2.[6,12] Formation of this so-called "Co−Mo−S" structure is known to dominate the catalytic activity of the system.[6] At higher Co loading (Co/Mo > 0.4), however, Co_9S_8 domains are formed that do not contribute significantly to the HDS activity. Ni can interact with MoS_2 in similar fashion, and there is evidence for a Ni−Mo−S phase.[12]

Chianelli et al.[4] proposed that Co or Ni adatoms increase the electron density at the Mo sites and that this results in stronger Mo−S bonds (and thus weaker C−S bonds), which leads to a higher HDS activity. Smit and Johnson,[5] however, have proposed that although Co and Ni do indeed contribute electron density to Mo, this transfer of electron density somewhat reduces the activity of Mo while greatly increasing the activity of the Co or Ni; in essence, MoS_2 can be viewed as a complex support for the highly active Co−Mo−S or Ni−Mo−S phase. Topsøe et al.[14] have shown that at the HDS active edges, coordinatively unsaturated Mo atoms must be formed by sulfur removal before HDS can take place. Recent STM studies on single-layer MoS_2 have shown that the S vacancies for the HDS can be generated by exposure to atomic hydrogen.[15]

The traditional synthesis of promoted MoS_2/Al_2O_3 catalyst is by simultaneous or successive impregnation of molybdenum and promoter salts onto alumina, followed by calcination (producing oxides), and sulfidation under the flow of H_2S in H_2 prior to use.[1,3−7] The HDS activity could be modified by using different molybdenum/promoter precursors, and also by changing the sequence of impregnation of molybdenum and promoter ions on alumina.

(1) (a) Furimsky, E. *Appl. Catal. A* **1998**, *171*, 177. (b) Grange, P. *Catal. Rev.-Sci. Eng.* **1980**, *21*, 135.
(2) (a) *Federal Register*, **2000**, August 4, *65* (151), 48057−48105. (b) *Chem. Eng. News* **2000**, *78* (1), 927.
(3) Prins, R.; de Beer, H. J.; Somorjai, G. A. *Catal. Rev.-Sci. Eng.* **1989**, *31*, 1.
(4) (a) Chianelli, R. R. *Catal. Rev.-Sci. Eng.* **1984**, *26*, 361. (b) Harris, S.; Chianelli, R. R. *J. Catal.* **1986**, *98*, 17. (c) Halbert, T. R.; Ho, T. C.; Stiefel, E. I.; Chianelli, R. R. *J. Catal.* **1991**, *130*, 116.
(5) Smit, T. S.; Johnson, K. H. *Catal. Lett.* **1994**, *28*, 361.
(6) Topsøe, H.; Clausen, B. *Catal. Rev.-Sci. Eng.* **1984**, *26*, 420.
(7) (a) Vasudevan, P. T.; Fierro, J. L. G. *Catal. Rev.-Sci. Eng.* **1996**, *38*, 161. (b) Ratnasamy, P.; Sivasanker, S. *Catal. Rev.-Sci. Eng.* **1980**, *22*, 401.
(8) (a) Dungey, K. E.; Curtis, M. D. *J. Am. Chem. Soc.* **1997**, *119*, 842. (b) Brito, J. L.; Barbosa, A. L. *J. Catal.* **1997**, *171*, 467.
(9) Bonneau, P. R.; Jarvis, R. F.; Kaner, R. B. *Nature* **1991**, *349*, 510.
(10) (a) Zdrazil, M. *Catal. Today* **1988**, *3*, 269. (b) Vicic, D. A.; Jones, W. D. *J. Am. Chem. Soc.* **1999**, *121*, 7606. (c) Afanasiev, P.; Xia, G. F.; Gilles, B.; Jouguet, B.; Lacroix, M.; *Chem. Mater.* **1999**, *11*, 3216.
(11) (a) Brenner, J.; Marshall, C. L.; Ellis, L.; Tomczyk, N.; Heising, J.; Kanatzidis, M. *Chem. Mater.* **1998**, *10*, 1244. (b) Cid, R.; Atanasova, P.; Cordero, R. L.; Palacios, J. M.; Agudo, A. L.; Olson, B. A.; *J. Catal.* **1999**, *182*, 328.
(12) (a) Bouwens, S. M. A. M.; Koningsberger, D. C.; de Beer, V. H. J.; Louwers, S. P. A.; Prins, R. *Catal. Lett.* **1990**, *5*, 273. (b) Ozkan, U. S.; Zhang, L.; Shuangyao, N.; Moctezuma, E. *J. Catal.* **1994**, *148*, 181.
(13) (a) Salmeron, M.; Somorjai, G. A.; Wold, A.; Chianelli, R. R.; Liang, K. S. *Chem. Phys. Lett.* **1982**, *90*, 105. (b) Kushmerick, J. G.; Weiss, P. S. *J. Phys. Chem. B* **1998**, *102*, 10094.
(14) (a) Topsøe, H.; Clausen, B. S.; Massoth, F. E. *Hydrotreating Catalysis, Science and Technology;* Springer-Verlag: Berlin, 1996. (b) Norskov, J. K.; Clausen, B. S.; Topsøe, H. *Catal. Lett.* **1992**, *13*, 1.
(15) Helveg, S.; Lauritsen, J. V.; Laegsgaard, E.; Stensgaard, I.; Norskov, J. K.; Clausen, B. S.; Topsøe, H.; Besenbacher, F. *Phys. Rev. Lett.* **2000**, *84*, 951.

10.1021/ja010516y CCC: $20.00
Published on Web 08/04/2001

The preparation of Mo-based supported catalyst with higher concentration of active metals on the exterior surface and high dispersion still represents a synthetic challenge in the field of advanced catalysis.[1−10] Alternative preparation methods involving metathesis reactions[9] and decomposition of metal sulfur compounds[10] have also been explored. These techniques appear to cause internal diffusion of active Mo into the support and produce ordered MoS_2 crystals with less edge density. While there are numerous studies on Co−Mo−S/Al_2O_3 and Ni−Mo−S/Al_2O_3 as HDS catalysts,[1−10] there are very few studies on the effect on HDS performance of double promotion by bimetallic Co−Ni modification of MoS_2/Al_2O_3,[16] and in fact, previous studies failed to find any significant enhancement compared to single promotion.

Recently, sonochemical reactions of volatile organometallics in an alkane medium have proven to be a unique technique to prepare high-surface-area nanophase metals, alloys, carbides, sulfides, nitrides, and supported catalysts.[17,18] In this study, we report a simple sonochemical synthesis, characterization, and kinetic studies of HDS activity of Co−Mo−S/Al_2O_3, Ni−Mo−S/Al_2O_3, and Co−Ni−Mo−S/Al_2O_3. The catalytic results are compared with the standard commercial catalysts.

Experimental Section

Materials and Equipment. Unless otherwise noted, all synthesis, preparation, and handling of the materials were done in an Ar atmosphere inert atmosphere box with O_2 < 0.5 ppm. Pentane was dried and distilled over Na/benzophenone and degassed prior to use. Isodurene (1,2,3,5-tetramethyl benzene, Aldrich) was dried and distilled over Na and degassed. Sulfur (99%), $Mo(CO)_6$ (98%), and $Co_2(CO)_8$ (stabilized with 1−5% hexanes) were purchased from Strem and used without further purification. Alumina (neutral 150 mesh, Aldrich) was heat treated at 400 °C under vacuum for 24 h to remove any adsorbed water. Thiophene (99% Aldrich) and dibenzothiophene (99%, Acros) were used without further purification. Industrial catalysts were obtained from Crosfield/ICI Catalysts. Crosfield 465 1/20 (Co/Mo oxides on γ-Al_2O_3: 10.6% Mo, 2.9%Co) and Crosfield 565 1/20 (Ni/Mo oxides on γ-Al_2O_3: 20.0% Mo, 3.7% Ni) were sulfided with 1:10 H_2S/H_2 flowing at 45 mL/min at 450 °C for 2 h prior to use. All sonications were done at 20 kHz using a Sonics & Materials VCX600 with a 1 cm^2 titanium horn and an acoustic intensity of ∼50 W cm^{-2} in a glass vessel under an argon atmosphere.

Reactions were analyzed with a Hewlett-Packard 6890 GC system equipped with an HP-5973 Mass Selective Detector fitted with a HP-5MS column. All SEM micrographs were obtained using a Hitachi S-4700 field emission SEM. All TEM micrographs were obtained using either a Phillips CM-12 microscope operating at 120 kV or a Vacuum Generators VG HB-501 STEM using a 6 Å probe and operating at 100 kV. XRD data were collected on a Rigaku D-max diffractometer using Cu Kα radiation. The XPS analysis was performed using a Physical Electronics Φ-5400 with a nonmonochromatized Mg Kα source (1253.6 eV), operating at 15 kV. The C(1s) peak at 284.6 eV was used to internally calibrate the binding energies. To avoid exposing the catalysts to air, a special transfer vessel was used to load the sample inside the inert atmosphere box and transfer it to the XPS specimen exchange chamber.

Synthesis of Sonochemical Co−Mo−S/Al_2O_3 Catalyst. The synthetic methodology is similar to our previous sonochemical synthesis of nanostructured MoS_2.[18] The Co promoter ions were also incorporated in the MoS_2 lattice sonochemically. In a typical preparation, sulfur (150 mg) is first dispersed in isodurene (35 mL) by short pulses of ultrasound followed by addition of 275 mg of $Mo(CO)_6$, 75 mg of $Co_2(CO)_8$, and 750 mg of γ-Al_2O_3. The vessel was sealed, transferred out of the inert atmosphere box, and sonicated under a flow of Ar for 1.5 h at 80 °C (60 °C bath temperature). The black slurry was then filtered inside the inert atmosphere box using a fine frit and washed several times with pentane. The washed powder was then heated to 80 °C under vacuum to remove any unreacted precursors and adsorbed solvent. The powder was annealed by heat treatment at 450 °C under a flow of 10% H_2 in He at 30 mL/min for 10 h using a single pass quartz microreactor, which also removes the excess sulfur. The elemental analysis gives a 5.5% Mo and ∼4.0% Co loading on alumina support. Similarly, sonochemical preparations were made of unpromoted MoS_2/Al_2O_3 and unsupported Co−Mo−S for comparison.

Synthesis of Sonochemical Ni−Mo−S/Al_2O_3 Catalyst. We have designed a different route to incorporate Ni in MoS_2/Al_2O_3 because volatile Ni precursors (e.g., $Ni(CO)_4$) are exceptionally toxic and dangerous to use.[19] Nickel coated on Al_2O_3 (Ni−Al_2O_3) has been used both as the Al_2O_3 support and as the source for Ni in the sonochemical preparation of Ni−Mo−S/Al_2O_3. To prepare Ni−Al_2O_3, γ-Al_2O_3 is first soaked in an aqueous solution of $Ni(N_2H_5)(N_2H_3COO)_3 \cdot H_2O$ complex for 1 h, dried in air, and heat treated under 10% H_2 in He at 300 °C for 2 h. $Ni(N_2H_5)(N_2H_3COO)_3 \cdot H_2O$ was synthesized and characterized according to methods outlined in the literature.[20] The sonochemical Ni−Mo−S/Al_2O_3 catalyst is then made by the same method as Co−Mo−S/Al_2O_3 by using Ni−Al_2O_3 (750 mg), $Mo(CO)_6$ (275 mg), and sulfur (150 mg). The initial sonochemical Ni−Mo−S/Al_2O_3 was annealed by heat treatment at 450 °C under a flow of 10% H_2 in He (30 mL/min) for 10 h using a single pass quartz microreactor. The sonochemically prepared catalyst typically has a 5.5% Mo and ∼2.8% Ni loading.

Synthesis of Sonochemical CoNi−Mo−S/Al_2O_3 Catalyst. For the preparation of CoNi−Mo−S/Al_2O_3, we use 3.5% Ni−Al_2O_3, $Mo(CO)_6$, $Co_2(CO)_8$, and sulfur. The sonochemical Co−Ni−Mo−S/Al_2O_3 catalyst is then made by the same method as Co−Mo−S/Al_2O_3 by using Ni−Al_2O_3 (750 mg), $Mo(CO)_6$ (275 mg), $Co_2(CO)_8$ (40 mg), and sulfur (150 mg). The initial sonochemical Ni−Mo−S/Al_2O_3 was annealed by heat treatment at 450 °C for 10 h under 10% H_2 in He flow (30 mL/min). The catalyst has a 5.5% Mo, 1.5% Co, and ∼2.5% Ni loading.

HDS of Thiophene. Catalytic studies of HDS of thiophene were performed at atmospheric pressure in a single-pass microreactor. The thiophene vapors were carried at a constant partial pressure of 75 mbar by a flow of hydrogen [flow rate = 23 cm^3(STP)/min]. The reaction products were analyzed with an on-line HP GC-MS and a 5730A HP GC fitted with a 9-ft *n*-octane/Porasil C column and a flame ionization detector.

HDS of Dibenzothiophene. DBT HDS was accomplished using a home-built stainless steel pressure vessel and sample withdrawal system. Catalyst (30−50 mg) was dispersed in 50 mL of decane containing 1% w:w dibenzothiophene (40 mM, 370 mg). The vessel was flushed with H_2 and pressurized to 3.4 MPa (500 psig) and heated to 375 °C during 1 h. For consistency, t_0 was denoted as the time when the target temperature was reached (at the end of ramping). In all cases, reactions reached equilibrium within 15 min after t_0. Samples were withdrawn in duplicate at 30, 45, 60, 75, and 90 min after t_0. The sampling system was equipped with a 2 μm stainless steel filter to prevent the removal of catalyst from the system. Aliquot size was about 0.25 mL. The samples were then centrifuged to remove any solid particulate, diluted 1:10 in pentane, and analyzed with GC-MS.

(16) (a) Guemez, M. B.; Cambra, J. F.; Arias, P. L.; Egia, B.; Uria, P. M.; Fierro, J. L. G. *Inf. Technol*. **1995**, *6*, 15. (b) Kameoka T.; Sato, T.; Yoshimura, Y.; Shimada, H.; Matsubashi, N.; Nishijima, A. *Sekiyu Gakkaishi* **1994**, *37*, 497.

(17) (a) Suslick, K. S. *Annu. Rev. Mater. Sci.* **1999**, *29*, 295. (b) Suslick, K. S. In *Handbook of Heterogeneous Catalysis*; Ertl, G., Knozinger, H., Weitkamp, J., Eds.; Wiley-VCH: Weinheim, 1997; Vol. 3, Chapter 8.6, pp 1350−1357. (c) Suslick, K. S.; Choe, S.-B.; Cichowlas, A. A.; Grinstaff, M. W. *Nature* **1991**, *353*, 414. (d) Grinstaff, M. W.; Salamon, M. B.; Suslick, K. S. *Phys. Rev. B* **1993**, *48*, 269. (e) Hyeon, T.; Fang, M.; Suslick, K. S. *J. Am. Chem. Soc.* **1996**, *118*, 5492. (f) Suslick. K. S.; Fang, M.; Hyeon, T. *J. Am. Chem. Soc.* **1996**, *118*, 11960. (g) Dhas, N. A.; Raj, C. P.; Gedanken, A. *Chem. Mater*. **1998**, *10*, 1446. (h) Dhas, N. A.; Gedanken, A. *Appl. Phys. Lett*. **1998**, *72*, 2514. (i) Dhas, N. A.; Gedanken, A. *J. Phys. Chem. B* **1997**, *101*, 3159. (j) Ashokkumar, M.; Grieser, F. *Rev. Chem. Eng.* **1999**, *15*, 41.

(18) Mdeleni, M. M.; Hyeon, T.; Suslick, K. S. *J. Am. Chem. Soc.* **1998**, *120*, 6190.

(19) Brauer, G. *Handbook of preparative inorganic chemistry*; Academic Press: New York, 1965; Vol. 2.

(20) (a) Ravindranathan, P.; Patil, K. C. *Ceram. Bull.* **1987**, *22*, 3261. (b) Dhas N. A.; Patil K. C. *J. Solid State Chem.* **1993**, *102*, 440.

Results and Discussion

Sonochemistry introduces a fundamentally different way of making materials by taking advantage of the intense energy within a collapsing bubble in a sound field.[16,21] A bubble expands and contracts in response to the negative and positive pressure induced by a sound field. The bubble grows larger during each cycle due to rectified diffusion and inertial growth. Once the bubble reaches a critical size, the next compression wave can create a violent collapse, the last stage of which is a near-adiabatic process. The temperatures during this stage reach upward of 5000 K with pressures above 300 atm.[22] In our experimental conditions, $Mo(CO)_6$ vapor in the bubble decomposes to give Mo atoms due to the local hot spots formed after bubble collapse. The hot Mo atoms coming out of the bubble react with the sulfur in the medium to form nanostructured MoS_2 (size ~3 nm)[17] and deposit on the alumina support as small clusters. The added $Co_2(CO)_8$ decomposes in a fashion similar to give Co atoms along with Mo atoms during the bubble collapse.

Nickel hydrazine carboxylate complex, $Ni(N_2H_5)(N_2H_3COO)_3 \cdot H_2O$, has been used as precursor for Ni for the preparation of sonochemical $Ni-Mo-S/Al_2O_3$. We were attracted by the low-temperature autocatalytic decomposition of the complex to yield pure nanocrystalline Ni (~3 nm) particles. A large amount of work has been carried out on decomposition of metal hydrazine carboxylate complexes under aerobic conditions for the synthesis of ultrafine particles of pervoskites and spinel metal oxides.[20] The fine particle nature of the oxide residue is due to the evolution of a large amount of gases during the decomposition of hydrazine carboxylate complexes. We have exploited this feature to prepare metallic clusters by decomposing the hydrazine carboxylate complex under a 1:10 H_2/He flow.

Characterization. The powder XRD of the sonochemical sample primarily showed the reflections of γ-Al_2O_3 with small broad peaks correspond to MoS_2. The nanostructured nature of the sonochemical MoS_2 particles causes the XRD line broadening and does not yield any information about the crystal structures of active components. SEM micrographs of sonochemically prepared catalysts show the MoS_2 particles made up of small spherical clusters as observed earlier for bulk sonochemical MoS_2.[17] Each spherical cluster is made up of finer particles of ~3 nm diameter, and the cluster rests atop a porous platelet of the alumina support. Representative micrographs of the sonochemical and commercial $Ni-Mo-S/Al_2O_3$ are shown in Figure 1. The SEM-XEDS analysis on the small spherical clusters showed increased signal intensity of the Mo compared to Al and O. This confirms our conclusion that in the sonochemically prepared catalysts, the small spherical clusters on the alumina support are indeed mostly MoS_2. The SEM morphologies of sonochemically prepared $Co-Mo-S/Al_2O_3$ and $Co-Ni-Mo-S/Al_2O_3$ are identical to the $Ni-Mo-S/Al_2O_3$. The elemental analysis and composition have also been examined using XEDS analysis coupled to SEM. The SEM-XEDS analysis profiles of sonochemically prepared catalyst are shown in Figure 2. The presence of Co and Ni has been confirmed by the characteristic signals of K lines at ~7 and ~7.5 keV, respectively. The L lines of Co and Ni can also be seen at ~1 keV. Unambiguous determination of sulfur and molybdenum were not possible on the SEM due to the overlap of the S K and Mo L lines at ~2.5 keV. The Mo K lines,

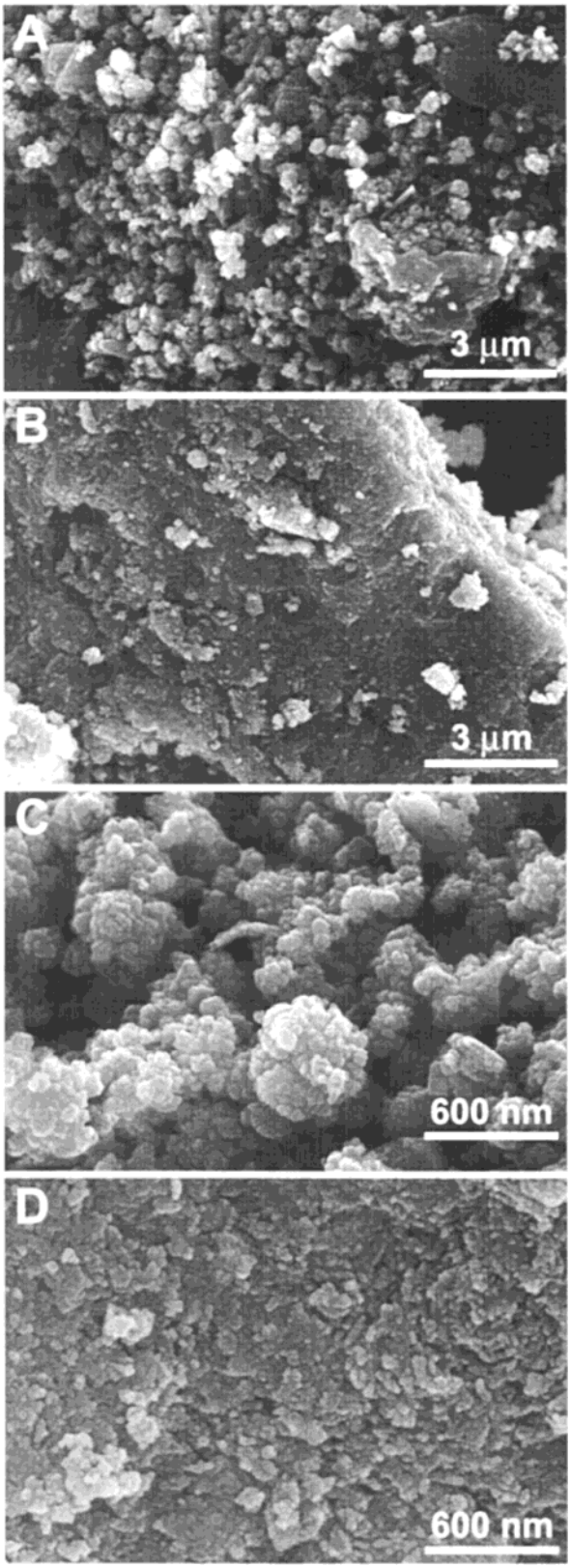

Figure 1. SEM micrograph of sonochemically prepared (A and C) and commercial $Ni-Mo-S/Al_2O_3$ (B and D). XEDS confirms that the numerous small clusters in the sonochemically prepared catalyst are Ni−Mo−S, whereas the occasional small clusters in the commercial catalyst (Crosfield) are Al_2O_3.

(21) (a) *Ultrasound: Its Chemical, Physical, and Biological Effects*; Suslick, K. S., Ed.; VCH Press: New York, 1988. (b) *Sonochemistry and Sonoluminescence*; Crum, L. A., Mason, T. J., Reisse, J. L., Suslick, K. S., Eds.; Kluwer Academic Publishers: Dordrecht, The Netherlands, 1999.

(22) (a) Flint, E. B.; Suslick, K. S. *Science* **1991**, *253*, 1325. (b) McNamara, W. B., III; Didenko, Y.; Suslick, K. S. *Nature* **1999**, *401*, 772. (c) McNamara, W. B., III; Didenko, Y.; Suslick, K. S. *J. Am. Chem. Soc.* **2000**, *122*, 8563. (d) McNamara, W. B., III; Didenko, Y.; Suslick, K. S. *Phys. Rev. Lett.* **2000**, *84*, 777.

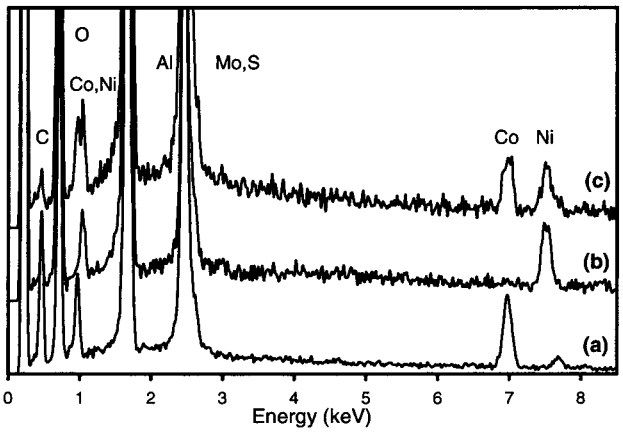

Figure 2. SEM-XEDS profiles of sonochemically prepared catalyst: (a) Co−Mo−S/Al_2O_3, (b) Ni−Mo−S/Al_2O_3, and (c) Co−Ni−Mo−S/Al_2O_3.

however, could be resolved at around 17.5 keV using high-resolution STEM-XEDS analysis (discussed below). The XEDS peak intensities were calibrated using a Cu grid for the calculation of elemental composition. The percentage of Mo is enhanced by 3-fold compared with the bulk elemental analysis values which indicate the surface enhancement of Mo (penetration depth under these conditions for XEDS ~4.5 μm). Therefore, the SEM-XEDS studies on sonochemically prepared catalysts confirm that the active component is indeed mostly on the exterior surface of the support.

The TEM of sonochemically prepared catalyst shows the lattice fringes of MoS_2 layers with interlayer spacing of ~6.2 Å, the same as those for bulk MoS_2.[23] The TEM shown in Figure 3 shows the microstructure of sonochemically prepared Co−Mo−S/Al_2O_3 and commercial Co−Mo−S/Al_2O_3 catalysts. The lattice fringes of MoS_2 are clearly seen on the surface of the support. Comparing TEM of the industrial and sonochemically prepared catalysts reveals an important difference: the industrial catalyst is mostly composed of multi-stacked and ordered layers with few wrinkled fringes, while the sonochemical Co−Mo−S catalyst shows short lengths of wrinkled layers that are highly disordered, and have only minimal layer stacking. The disordered, fractured, and defective nature of sonochemically prepared MoS_2 layers are inherent in having clusters made up of nanometer sized, highly dispersed MoS_2 particles. The sonochemically prepared MoS_2 has increased edge density and higher dispersion, both of which are desirable for HDS activity. Similarly layered MoS_2 structures are also observed for the sonochemically prepared Ni−Mo−S/Al_2O_3 and Co−Ni−Mo−S/Al_2O_3.

The electronic states of metals and sulfur in the catalyst were probed by X-ray photoelectron spectroscopy (XPS).[24] XPS of the sonochemically prepared catalyst showed that the Mo is concentrated at the surface (X-ray penetration depth ~50 Å). The XPS signal intensities were corrected with sensitivity factors for the calculations of atomic concentration. The atomic concentration calculations indicated that there is a 5-fold enhancement of surface Mo versus the bulk material for the sonochemically prepared catalyst. On the other hand, the commercial catalyst did *not* show Mo surface enhancement in XPS.

Table 1 summarizes the XPS binding energies (BE) of Mo, Co, Ni, and S of sonochemical Co−Mo−S/Al_2O_3, Ni−Mo−S/Al_2O_3, and Co−Ni−Mo−S/Al_2O_3, as well as binding energy differences ΔE_1 and ΔE_2 (which are obtained by subtracting the BE of M($2p_{3/2}$) (M = Co, Ni) and Mo($3d_{5/2}$) from the S($2p_{3/2}$), respectively). The XPS BE, ΔE_1, and ΔE_2 values of unsupported sonochemical Co−Mo−S and commercial supported samples are also included in Table 1 for comparison.

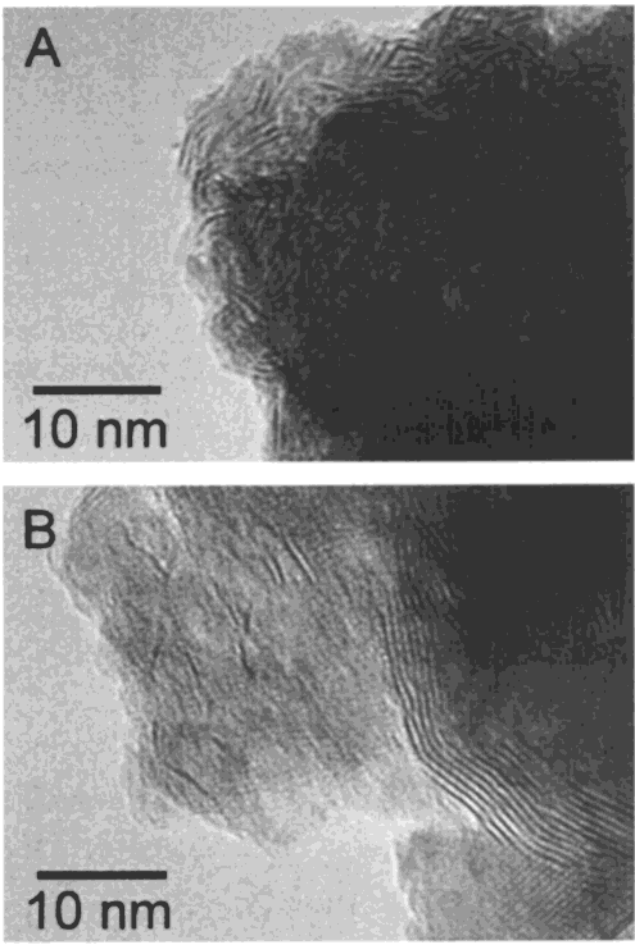

Figure 3. TEM images: (A) sonochemical Co−Mo−S/Al_2O_3 and (B) commercial (Crosfield) Co−Mo−S/Al_2O_3.

It is known that Co interacts with the Al_2O_3 support due to the facile formation of spinel $CoAl_2O_4$ oxide phase; the spinel phase actually decreases HDS activity.[6] The BE of sonochemical unsupported Co−Mo−S and supported Co−Mo−S/Al_2O_3 is identical, indicating a negligible interaction between the support and cobalt under the sonochemical samples. This is further supported by BE values of a commercial carbon supported catalyst (Co−Mo−S/C), which are identical to those of supported and unsupported sonochemically prepared catalysts. The peak positions of M, Mo, and S in the sonochemically prepared catalyst are in good agreement with the conventional samples.[25]

We also performed STEM-XEDS spot analysis on the sonochemical samples to determine if the promoter-metal and Mo atoms coexist spatially or if they phase segregate. Figure 4a shows a STEM micrograph of sonochemical Ni−Mo−S/Al_2O_3 catalyst. The circles represent the locations and the areas of analysis. Analysis was done both on and off MoS_2 fringes ("on-fringe" and "off-fringe", respectively), and the intensities

(23) Inamura, K.; Prins, R. *J. Catal.* **1994**, *147*, 515.

(24) Moulder J. F.; Stickle, W. F.; Sobol, P. E.; Bomben, K. D. *Handbook of X-ray Photoelectron Spectroscopy*; Chastain J., Ed.; Perkin-Elmer: Eden Prairie, MN, 1992.

(25) (a) Alstrup, I.; Chorkendorff, I.; Candia, R.; Clausen, B. S.; Topsøe, H. *J. Catal.* **1982**, *77*, 397. (b) Bouwens, S. M. A. M.; van Zon, F. B. M.; van Dijk, M. P.; van der Kraan, A. M.; de Beer, V. H. J.; van Veen, J. A. R.; Koningsberger, D. C. *J. Catal.* **1994**, *146*, 375.

Table 1. XPS Binding Energy Values for Sonochemically Prepared Catalysts

	Co−Mo−S unsupported	Co−Mo−S /Al_2O_3[a]	Ni−Mo−S /Al_2O_3[a]	Co−Ni−Mo−S /Al_2O_3	Co−Mo−S /C[b]
M (Co, Ni) $2p_{3/2}$	778.6	778.6 (778.6)	853.6 (852.8)	778.6, 853.5	778.6
S $2p_{3/2}$	162.4	162.5 (161.2)	162.6 (162.1)	162.5	162.5
ΔE_1 (M $2p_{3/2}$ − S $2p_{/32}$)	616.2	616.1 (617.4)	691.0 (690.7)	616.1, 691.0	616.1
Mo $3d_{5/2}$	229.1	229.0 (228.1)	229.2 (228.8)	229.2	229.1
ΔE_2 (Mo $3d_{5/2}$ − S $2p_{/32}$)	66.7	66.5 (66.9)	66.6 (66.7)	66.7	66.7

[a] Values determined for the equivalent conventional catalyst (ref 25) are given in parentheses. [b] Reference 25.

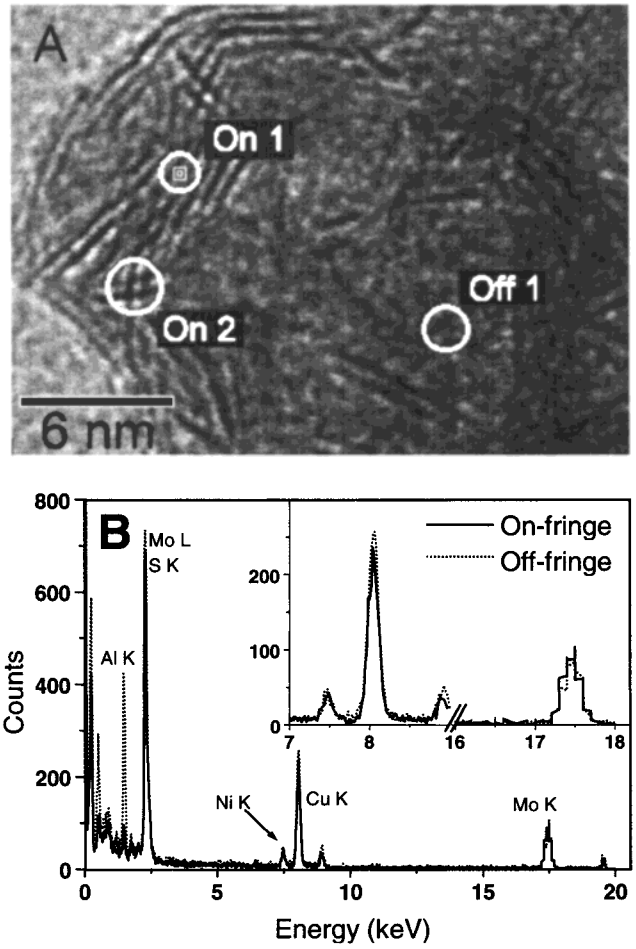

Figure 4. (A) STEM of sonochemically prepared Ni−Mo−S/Al_2O_3 showing MoS_2 lattice fringes and displaying the areas of analysis. (B) Spot XEDS analysis on and off fringes for Ni−Mo−S/Al_2O_3 scaled to Mo K intensity. The inset shows an enlarged view of Ni K/Cu K and Mo K regions.

of Mo Kα (17.5 eV), Ni Kα (7.5 eV), and Al Kα (1.5 eV) were determined. For comparison purposes, the intensities of the spectra were scaled based on the Mo Kα peak intensity. Within the scope of this analysis, there were no significant changes in the intensity of Mo Kα versus the Ni Kα peak. XEDS overlay spectra (Figure 4b) shows the presence of Mo, Ni, and S in the on-fringe spot. The only change observed that depended on location was the intensity of the Al Kα peak, which is very weak on-fringe. We have obtained similar results in sonochemical Co−Mo−S/Al_2O_3 and Co−Ni−Mo−S/Al_2O_3. The XEDS spot analyses of the sonochemical samples on-fringe and off-fringe indicate that the Co or Ni promoters and Mo are uniformly distributed on the alumina sample. The XEDS results were consistent with the STEM electron probe mapping analysis of the sonochemically prepared catalysts.

HDS of Thiophene. The specific surface areas of the pretreated sonochemical and commercial catalysts were ∼170 and ∼220 m^2/g, respectively, but this simply reflects the total surface area of the support. Given the different degree of dispersion for sonochemical and industrial catalysts and the fact that the active sites are located at the edges of MoS_2 layers, activity is normalized to the mass of metal,[26,27] rather than to the surface area. The stability of the sonochemical and commercial catalysts was measured over the course of 5 days by continuous HDS of thiophene using a single-pass microreactor at 400 °C. Figure 5 displays the turnover frequencies as function of catalytic use over time. The stabilities of the promoted sonochemically prepared catalysts were calculated using a first-order exponential fit after reaching a steady state conversion (60 h). The half-lives for the sonochemically prepared catalysts are around 25 days, comparable to the commercial catalyst. In addition, the sonochemically prepared catalysts can be easily regenerated at 450 °C for 10 h under 10% H_2 in He flow and return to nearly their initial activity.

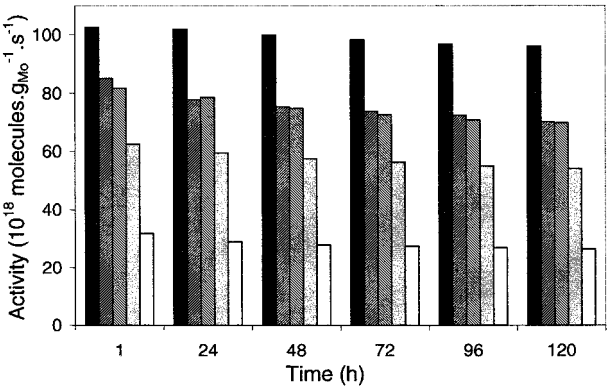

Figure 5. Longevity of catalytic activity for hydrodesulfurization of thiophene at 400 °C. From left to right at each time: sonochemically prepared CoNi−Mo−S/Al_2O_3; sonochemically prepared Co−Mo−S/Al_2O_3; Ni−Mo−S/Al_2O_3, treated thermally with H_2 in He; commercial (Crosfield) Co−Mo−S/Al_2O_3; and commercial (Crosfield) Co−Mo−S/Al_2O_3.

As is seen in Figure 5 (and discussed below), the sonochemical Co−Ni−Mo−S/Al_2O_3 catalyst shows higher activity for HDS of thiophene than the Co or Ni promoted sonochemical and commercial catalysts. The variation of catalytic activity as a function of Co wt % in Co−Ni−Mo−S/Al_2O_3 is shown in Figure 6. The activity values plotted here were measured after 60 h of use. As the concentration of Co promoter increases in Co−Ni−MoS/Al_2O_3, the catalytic activity increases to an optimum composition of 2% Co and 2.8% Ni.

It is worth mentioning that the HDS activity of Ni and Co promoted sonochemically prepared catalyst is higher after thermal treatment with 10% H_2 in He than if treated only with He. This is most likely because H_2 removes sulfur atoms from the edges of the Co−Mo−S or Ni−Mo−S structures, resulting in coordinatively unsaturated Mo and promoter atoms that are more active catalytic sites for HDS.[28]

(26) Pecoraro, T. A.; Chianelli, R. R. *J. Catal.* **1981**, *67*, 430.
(27) Ramanathan, S.; Oyama, S. T. *J. Phys. Chem.* **1995**, *99*, 16365.
(28) Byskov, L. S.; Norskov, J. K.; Clausen, B. S.; Topsøe, H. C. *Prepr. Am. Chem. Soc., Div. Pet. Chem.* **1998**, *43*, 12.

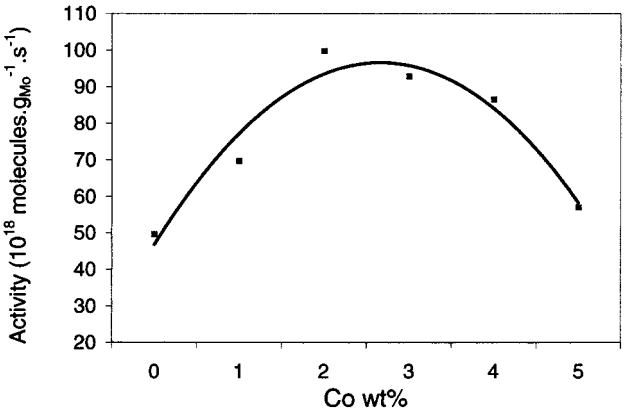

Figure 6. Variation of catalytic activity for thiophene hydrodesulfurization as a function of Co amount in sonochemically prepared Co−Ni−Mo−S/Al_2O_3.

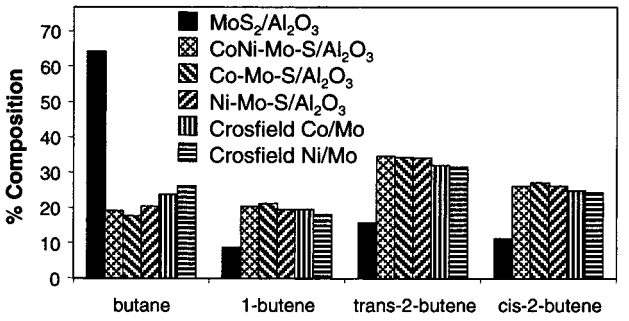

Figure 7. Product distribution of thiophene hydrodesulfurization.

Scheme 1

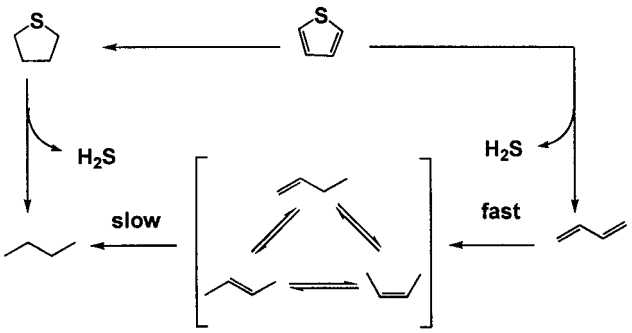

The principal products detected by GC-MS were the C_4 hydrocarbons: butane, 1-butene, *trans*-2-butene, and *cis*-2-butene (Figure 7). We do not see butadiene due to the high reactivity of the catalyst (40% conversion); the amount of tetrahyrothiophene in the product is <0.2%. The promoted catalysts show high selectivity for butenes compared with the unpromoted MoS_2, which gives more butane. In the absence of promoters the butadiene or thiophene strongly adsorbs on MoS_2 and undergoes extensive hydrogenation.[29] On the basis of the observed products, a plausible mechanism for thiophene HDS would involve initial homolytic cleavage of the thiophene C−S bond and hydrogenolysis to give H_2S and butadiene. Butadiene undergoes rapid hydrogenation to 1-butene, which is subsequently hydrogenated slowly to butane or isomerized to a thermodynamic mixture of *cis*- and *trans*-2-butenes (Scheme 1).[30,31] Tetrahydrothiophene can also undergo HDS to give butane.

HDS of Dibenzothiophene. Analysis of the aliquots withdrawn from the pressure vessel during the reaction shows a linear decrease in the concentration of dibenzothiophene (DBT) over time. This indicates zero order kinetics, observed when the substrate concentration is high and turnover is determined by the availability of active sites on the catalyst. Figure 8 shows specific activity of each catalyst measured as molecules of DBT consumed per gram of metal per minute.

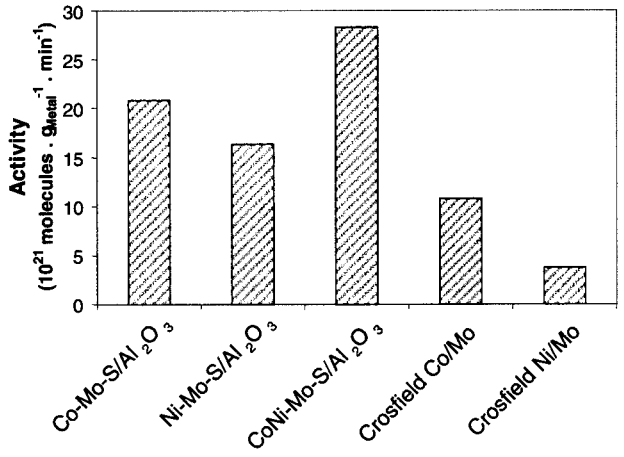

Figure 8. Specific activity for dibenzothiophene hydrodesulfurization by sonochemical and commercial (Crosfield) catalysts.

Comparing sonochemically prepared catalysts to industrial ones, it is clear that sonochemically prepared catalysts are superior for HDS of DBT. The sonochemical Co−Mo−S/Al_2O_3 is more active than the sonochemical Ni−Mo−S/Al_2O_3, and they are about two and four times more active than their commercial counterparts, respectively. The enhancements in activity of the sonochemically prepared catalyst could be due to improved mass transport since the active species are predominantly on the outside surface of the alumina support. The beneficial effect on the HDS performance of Co−Ni−Mo−S/Al_2O_3 is probably due to the different stages and nature of incorporation of Co and Ni to MoS_2.

Product distribution afforded by an HDS catalyst is also of importance. Numerous studies have been carried out on coordination of DBT and other thiophenic species on model catalysts.[32−36] Dibenzothiophene adsorbed on the catalyst can undergo either hydrodesulfurization or hydrogenation. Scheme 2 shows the general pathways for DBT reactions. The two major products of hydrodesulfurization of DBT are biphenyl (BP) and cyclohexylbenzene (CHB). BP is the direct HDS product and is desired due to its commercial application and smaller hydrogen consumption, while CHB is a product of HDS of tetrahydrodibenzothiophene (TH-DBT), which itself is an incomplete hydrogenation product of DBT. Classic experimental and theoretical work by Chianelli, Daage, and Murray have shown that HDS can happen on the rim and edge sites of a multilayer MoS_2 catalyst, while hydrogenation probably only happens on the rim sites.[32,33] Furthermore, selectivity [CHB]/[BP] is greatly dependent on partial pressure of H_2 and temperature.[37] High temperatures and H_2 pressures yield more CHB. The product distribution of sonochemically prepared

(29) Jayamurthy, M.; Vasudevan, S. *J. Phys. Chem.* **1994**, *98*, 6777.
(30) Benson, J. W.; Schrader, G. L.; Angelici, R. J. *J. Mol. Catal. A: Chemical* **1995**, *96*, 283.
(31) Luo, S.; Rauchfuss, T. B.; Gan, Z. *J. Am. Chem. Soc.* **1993**, *115*, 4943.
(32) Daage, M.; Murray, H. H. *Prepr. Am. Chem. Soc., Div. Pet. Chem.* **1993**, *38*, 660.
(33) Daage, M.; Chianelli, R. R. *J. Catal.* **1994**, *149*, 414.
(34) Rauchfuss, T. B. *Prog. Inorg. Chem.* **1991**, *30*, 259.
(35) Tarbuck, T. L.; McCrea, K. R.; Logan, J. W.; Heiser, J. L.; Bussell, M. E. *J. Phys. Chem. B* **1998**, *102*, 7845.
(36) Diemann, E.; Weber, T.; Müller, A. *J. Catal.* **1994**, *148*, 288.

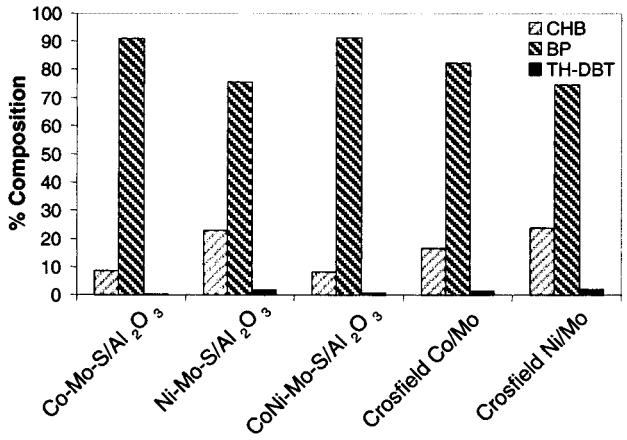

Figure 9. Product distribution of dibenzothiophene hydrodesulfurization: CHB, cyclohexylbenzene; BP, biphenyl; and TH-DBT, tetrahydrodibenzothiophene.

Scheme 2

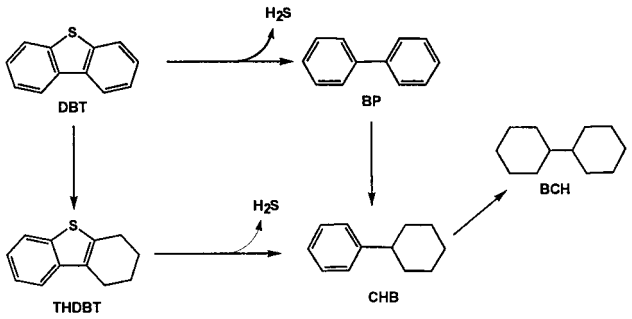

catalyst was nearly identical or slightly better than that of the industrial catalyst (Figure 9). All of the product distribution measurements were obtained at 74% DBT conversion. For all catalysts studied, BP was the major product, although the Co-promoted catalysts were more selective than the Ni-promoted ones. The amount of TH-DBT also reflected catalyst selectivity. In the case of Co catalysts, TH-DBT only constituted 1.0−1.3% of the total product, while for the Ni catalyst, the amount was ∼1.9%. In all cases, complete hydrogenation products such as bicyclohexane accounted for less than 0.3% of products.

(37) Singhal, G. H.; Espino, R. L.; Sobel, J. E.; Huff, G. A. *J. Catal.* **1981**, *67*, 457.

Conclusion

Co, Ni, and Co−Ni promoted molybdenum sulfide on alumina catalysts have been generated ultrasonically using molybdenum carbonyl, elemental sulfur, dicobalt octacarbonyl, and Al_2O_3 (or nickel on Al_2O_3). TEM studies demonstrated that the sonochemical technique enhances the dispersion of MoS_2 layers on the alumina support compared to the conventional, commercial catalyst (Crosfield). SEM-XEDS and XPS studies have shown that the Mo is mostly concentrated on the surface of alumina in the case of the sonochemically prepared catalysts, but *not* for conventionally prepared catalysts. STEM-XEDS spot analysis showed that Mo is not phase segregated from the promoter metals (Co, Ni, and Co−Ni) on the scale of ∼3 nm, indicating the formation of binary metal sulfide M−Mo−S structures. The HDS activity of sonochemical Co promoted MoS_2/Al_2O_3 is slightly higher than that of the Ni counterpart, and they are 2-fold times and 3-fold times more active than their respective commercial counterparts. The bimetallic Co−Ni promoted MoS_2/Al_2O_3 has HDS activity 3-fold and 7-fold times better than the commercial Co−Mo−S/Al_2O_3 and Ni−Mo−S/Al_2O_3 catalysts, respectively. The superior HDS activity of sonochemical MoS_2 catalysts is likely to arise from the higher dispersion of the MoS_2 on the support and the consequent higher concentration of the catalytically active edge sites.

Acknowledgment. These studies were supported by the NSF (CHE-0079124). Surface and electron microscopic analyses were carried out in the UIUC Center for Microanalysis of Materials, which is supported by the U.S. Department of Energy, Division of Materials Sciences under Award No. DEFG02-ER9645439, through the Frederick Seitz Materials Research Laboratory at the University of Illinois at Urbana-Champaign. The assistance of Drs. Ray Twesten and Rick Haasch of the Center for Microanalysis of Materials is appreciated. The authors also wish to thank Dr. Robert Quigley of Crosfield/ICI for the generous donation of the Crosfield catalysts.

JA010516Y